X-626-74-305
PREPRINT

NASA TM X- 70779

PROTONS AS THE PRIME CONTRIBUTORS TO THE STORM TIME RING CURRENT

(NASA-TM-X-70779) PROTONS AS THE PRIME CONTRIBUTORS TO THE STORM TIME RING CURRENT (NASA) 19 p HC $3.25 CSCL 20H
N75-11722
Unclas
G3/72 02697

F. W. BERKO
L. J. CAHILL, JR.
T. A. FRITZ

OCTOBER 1974

GSFC
GODDARD SPACE FLIGHT CENTER
GREENBELT, MARYLAND

For information concerning availability
of this document contact:

Technical Information Division, Code 250
Goddard Space Flight Center
Greenbelt, Maryland 20771

(Telephone 301-982-4488)

PROTONS AS THE PRIME CONTRIBUTORS TO STORM TIME RING CURRENT

F. W. Berko
Goddard Space Flight Center, Greenbelt, Md. 20771

L. J. Cahill, Jr.
University of Minnesota, Minneapolis, Minn. 55455

T. A. Fritz
NOAA/SEL, Bounder, Colorado 80302

Following a large sudden commencement on 17 June 1972, a large magnetic storm evolved, with a well-developed main phase and recovery phase. Explorer 45 (S^3-A), with its apogee near 16 hours local time in June, measured the equatorial particle populations and magnetic field throughout this period. Using data obtained during the symmetric recovery phase, it is shown that, through a series of self-consistent calculations, the measured protons, with energies from 1 keV to 872 keV, can account for the observed ring current magnetic effects within experimental uncertainties. This enables us to set an upper limit to the heavy ion contribution to the storm time ring current of a few percent of the proton contribution.

Introduction

Explorer 45 was launched into an elliptical, equatorial orbit on 15 November, 1971. It carried a variety of instruments which made extensive measurements of the ring current and other phenomena in the inner magnetosphere (Longanecker and Hoffman, 1973). Initial data from Explorer 45 have been presented showing magnetic field measurements (Cahill, 1973), ring current particle distributions (Smith and Hoffman, 1973), and proton energy spectra and pitch angle distributions (Konradi et al., 1973). Hoffman (1973) has presented simultaneous particle and magnetic field data obtained by S^3-A during the December 1971 magnetic storm period.

Data from the Explorer 45 satellite will be used in this paper to calculate the deformation of the geomagnetic field due to ring current protons, using the self-consistent technique of Hoffman and Bracken (1967). Previously, using the Hoffman and Bracken calculation method, Hoffman and Cahill (1968) used Explorer 26 magnetometer data to derive a ring current particle distribution which gave good agreement with the magnetic observations. Prior to Explorer 45 ring current measurements, only one case of direct observations of the storm-time ring current particle system was reported (Frank, 1967). Smith and Hoffman (1974) have recently discussed several cases of storm-time ring current particle measurements made by the S^3-A satellite in the dusk hours. Data to be used in this study were collected when the spacecraft apogee was at about 16 hours MLT.

Magnetic Conditions and Requirements

The first figure presents the equatorial Dst values for June 17 -

20, 1972, with day and time indicated on the bottom and the S^3-A satellite orbit numbers during this time indicated along the top. As is evident from the figure, this magnetic storm was characterized by a very large main phase, with Dst reaching a minimum value of -190γ; and a long recovery phase extending at least one day past the end of the figure. To perform the ring current calculations to be described, we sought a time period when the following conditions prevailed:

i) The proton energy density measured on the inbound and outbound portions of the (7 + hour) orbit were symmetric;

ii) The satellite orbit remained very close (i.e. within $\pm 1^{\circ}$) to the magnetic equator;

iii) The satellite apogee was on the dayside;

iv) The ΔB profile obtained from the onboard magnetometer was essentially symmetric on the outbound and inbound portions of the orbit, implying the existence of a symmetric ring current.

Orbit 676, on June 19, satisfied all these requirements, and data from this orbit will be used in this study. These data were obtained during the symmetric recovery phase, at a time of little substorm activity. Measurements made during substorms showed more complicated effects (Williams et al., 1974) and are unsuitable for the calculations to be performed here.

Particle and Magnetic Observations

Figure 2 presents the differential energy spectra at three L values for 1 kev to 872 kev protons during orbit 676. The spectra are averaged over both outbound and inbound data obtained at L values of 2.5, 3.5 and 4. Note first that the maximum energy density was at L = 3.5. Energy spectra for L = 3.5 and 4 are quite similar. They both decrease fairly uniformly from 1 kev to about 120 kev, then decrease very rapidly at energies above 120 kev. At L = 2.5 the spectrum is considerably less intense and decreases more rapidly up to about 220 kev than the other two spectra, but then remains essentially flat up to the maximum energy of 872 kev.

Pitch angle distributions of the measured protons are presented in Figure 3 at L values of 2.5, 3.5 and 4 for data obtained both on the outbound (circles) and inbound (triangles) portions of orbit 676. The distributions at each L value were then fit to a function of the form $\sin^n\alpha$. At L = 2.5, n had the value 2.3, while at L = 4, n was 1.3. It was determined that n varied linearly from L = 2.5 to L = 4, and then n remained approximately constant at 1.3 for L values greater than 4, (at least out to S^3-A apogee at L = 5.2 and 16 hours local time).

Measured proton energy densities over the range 1 kev to 872 kev from inbound and outbound portions of orbit 676 were integrated over energy and pitch angle and then averaged. The resulting values are plotted as a function of L in Figure 4. A smooth, continuously differentiable function composed of a combination of exponentials and fifth-order polynomials was then fit to the data, with special attention given to fitting the data both in value and slope near the maximum energy density at L = 3.5. This function is shown as the solid curve in figure 4, and is seen to fit measurements very well at L values from 3 to 4.8.

Inbound and outbound magnetometer values were averaged to obtain the (dashed) curve shown in Figure 5 as the measured ΔB (see e.g. Cahill, 1973; Hoffman, 1973). There was a slight asymmetry in measured ΔB at the minimum value near L = 3.4. On the outbound pass the minimum value was approximately -115 gammas; inbound it was approximately -130 gammas. ΔB is defined as

$$\Delta B = \left| \vec{B}_{measured} \right| - \left| \vec{B}_{model} \right|$$

Calculational Approach

The smooth energy density profile of figure 4 and the pitch angle distributions presented above were then used to calculate the magnetic effects of the proton ring current in a self-consistent manner (see Hoffman and Bracken, 1967):

i) The proton energy density and pitch angle distributions were placed in a model magnetic field composed of a main (spherical harmonic expansion) field plus boundary and neutral sheet effects. The current resulting from these particles in this field model produced a 1st order magnetic field, from which was obtained a first order ΔB.

ii) This 1st order ring current field was added vectorially to the (original) model field. A 2nd order ring current was then calculated in this 1st order field from the measured proton energy density, and then a 2nd order ring current field was computed.

iii) This procedure was repeated until self-consistency was attained, that is when ΔB (n^{th} order) was essentially equal to ΔB ($n + 1^{st}$ order). In this case, the 3^{rd} and 4^{th} order ΔB differed by less than 1%.

Both the 1^{st} and 3^{rd} order ΔB profiles are shown in Figure 5. Differences between the measured and 3^{rd} order calculated ΔB are less than 10% from L = 2 to L = 5, and can be accounted for largely by uncertainties in the measurements and inaccuracies in the fit to the measured energy density profile (figure 4).

DISCUSSION

We have shown that, within experimental uncertainties and inaccuracies to the fitted data, we can account for the observed ΔB with the measured count rates. However, one must consider the possibility that at least some of the counts recorded in our particle detectors might have been due to heavy ions. Shelley et al., (1972) have reported observations of heavy ions from low altitude spacecraft, and have suggested that these heavy ions could make "... a substantial contribution to the storm-time magnetic-field depression (Dst)...", noting that, for the same proton and oxygen fluxes, the O^+ energy density is 4 times the proton energy density. More recently, Johnson et al. (1974) have reported fluxes of He^+ ions, also observed at low altitudes, that are not insignificant, and which they believe to be of ionospheric origin.

Thus, it is of interest to examine what the S^3-A megnetic and particle data can say with regard to the heavy ion contribution to the ring current during orbit 676. If we assume that 5% of the counts in the particle detectors were due to heavy ions (O^+), and further that these ions had the same pitch angle distribution as the protons, then the energy density curve in Figure 4 would be increased by 15%. It follows then that using this higher value for the energy density in the same type of self-consistent calculation, we should arrive at values of ΔB which are about 12% greater than those calculated using the original energy density profile. At this point, we must examine the uncertainties that exist in the "measured ΔB".

Uncertainties in the magnetometer measurements, due to averaging over time and inbound and outbound data, are on the order of 5γ. In the determination of the measured ΔB curve, a model field was used, from which the measurements were subtracted. The absolute validity of this model field will not be discussed here, but its relative accuracy is important. The model used is based on measurements made under a variety of magnetic conditions. It has several adjustable parameters (i.e. subsolar distance of the magnetopause, epoch) which have effects on the magnitude of the field it returns at any given L, latitude and longitude. Variations in these parameters can change the model field values by as much as 10γ in the ring current region. Thus, the combined uncertainty in the measured ΔB profile is of the order of 15γ. Consequently, a change of about 12% in the calculated, self-consistent ΔB is within the uncertainty which we can assign to the measured ΔB.

Although the field model used for the ring current calculations includes effects of distributed currents in the magnetosphere (Olson, 1974), the model used for determining the measured ΔB does not. However, since we have chosen primarily dayside data, effects of neutral sheet and tail current fields are minimal, and the greatest effects of magnetopause currents are at L = 5, decreasing at smaller L values.

We can therefore place an upper limit to the ion flux in the ring current region at a few percent of the proton flux at the time of orbit 676. A confirmation of the low heavy ion contribution is also indicated by the low O^+ precipitation observed at this time by the 1971-089A mass spectrometer (R. D. Sharp, private communication, 1974). It should be noted that earlier in this storm, during the asymmetric phase, definite O^+ and He^+ precipitation was observed in the 1971 - 089A data.

CONCLUSIONS

We have shown that when the satellite orbit was equatorial during a magnetic storm recovery phase and the magnetometer indicated the existence of a symmetric ring current, the measured proton energy density could be used to calculate a ΔB profile which is in good agreement with the measured profile. As a corollary, we can therefore place an upper limit to the ion flux in the ring current region at a few percent of the proton flux,

ACKNOWLEDGEMENTS

We are pleased to acknowledge the helpful discussions and beneficial criticisms from R. A. Hoffman and P. H. Smith. R. D. Sharp made many helpful suggestions in a critical reading of the manuscript.

REFERENCES

Cahill, L. J., Jr., Magnetic Storm Inflation in the Evening Sector, JGR, 78, 4724-4730, 1973.

Frank, L. A., On the Extra-terrestrial Ring Current During Geomagnetic Storms, JGR, 72, 3753-3767, 1967.

Hoffman, R. A., Particle and Field Observations from Explorer 45 During the December 1971 Magnetic Storm Period, JGR, 78, 4771-4777, 1973.

Hoffman, R. A., and Bracken, P. A., Higher-order Ring Currents and Particle Energy Storage in the Magnetosphere, JGR, 72, 6039-6049, 1967.

Hoffman, R. A., and Cahill, L. J., Jr., Ring Current Particle Distribution Derived from Magnetic Field Measurements, JGR, 73, 6711-6722, 1968.

Johnson, R. G., Sharp, R. D., and Shelley, E. G., The Discovery of Energetic He^+ Ions in the Magnetosphere, J. Geophys. Res., 79, 3135-3139, 1974.

Konradi, A., Williams, D. J., and Fritz, T. A., Energy Spectra and Pitch Angle Distributions of Storm-time and Substorm Injected Protons, JGR, 78, 4739-4744, 1973.

Longanecker, G. W., Hoffman, R. A., S^3-A Spacecraft and Experiment Description, JGR, 78, 4711-4717, 1973.

Olson, W. P., A Model of the Distributed Magnetospheric Currents, J. Geophys. Res., 79, 3731-3738, 1974.

Shelley, E. G., Johnson, R. G. and Sharp, R. D., Satellite Observations of Energetic Heavy Ions During a Geomagnetic Storm, JGR, 77, 6104-6110, 1972.

Smith, P. H. and Hoffman, R. A., Ring Current Particle Distributions During the Magnetic Storms of December 16-18, 1971, J. Geophys. Res., 78, 4731-4737, 1973.

Smith, P. H. and Hoffman, R. A., Direct Observations in the Dusk Hours of the Characteristics of the Storm Time Ring Current Particles During the Beginning of Magnetic Storms, JGR, 79, 966-971, 1974.

Williams, D. J., Barfield, J. N. and Fritz, T. A., Initial Explorer 45 Substorm Observations and Electric Field Considerations, JGR, 79, 554-564, 1974.

FIGURE CAPTIONS

Figure 1: Equatorial values of D_{ST} for the period 17 to 20 June, 1972. S^3-A orbit numbers are shown at the top.

Figure 2: Differential energy spectra averaged over inbound and outbound data at three L values.

Figure 3: Pitch angle distributions at three L values for both outbound and inbound data during orbit 676.

Figure 4: Proton energy densities integrated over energy and pitch angle and averaged over inbound and outbound portions of orbit 676; a smooth, differentiable function fit to these data is shown as the solid curve.

Figure 5: Measured ΔB (dashed curve) and 1st and 3rd order calculated ΔB profiles.

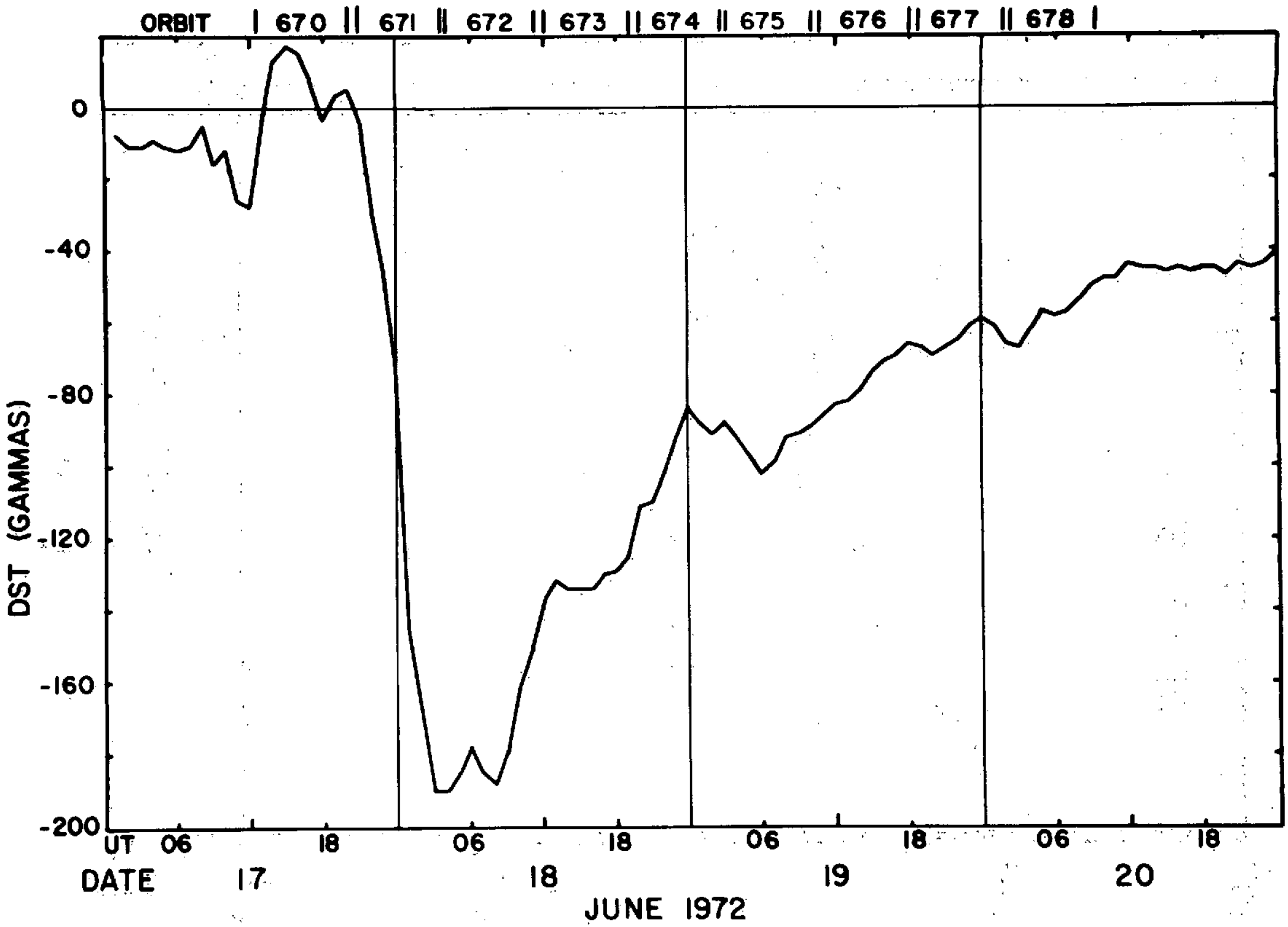
ORBIT | 670 || 671 || 672 || 673 || 674 || 675 || 676 || 677 || 678 |
0
-40
-80
-120
-160
-200
DST (GAMMAS)
UT 06 18 06 18 06 18 06 18
DATE 17 18 19 20
JUNE 1972

Figure 1

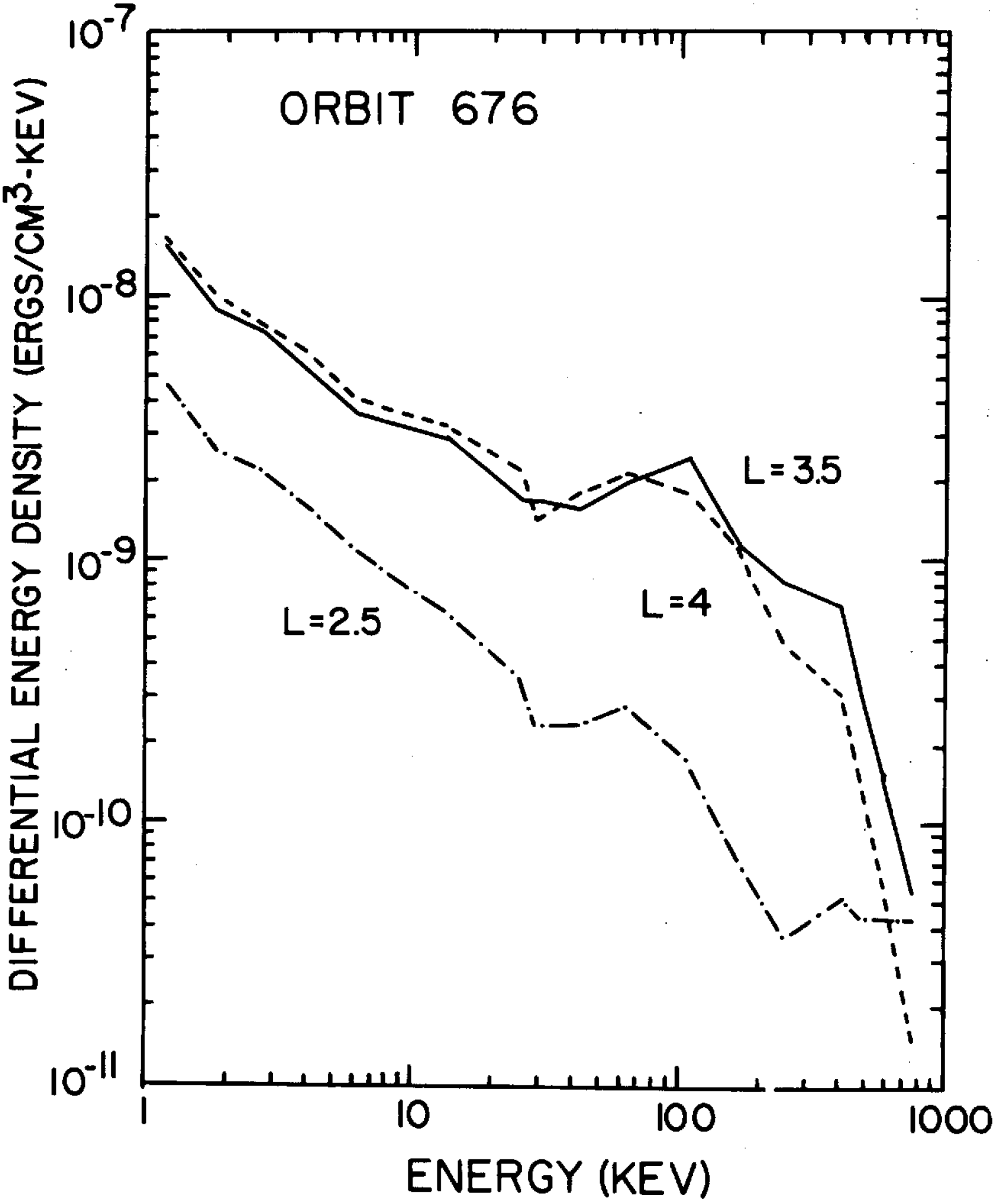
ORBIT 676
DIFFERENTIAL ENERGY DENSITY (ERGS/CM3-KEV)
ENERGY (KEV)
L=3.5
L=4
L=2.5
10-7
10-8
10-9
10-10
10-11
1
10
100
1000

Figure 2

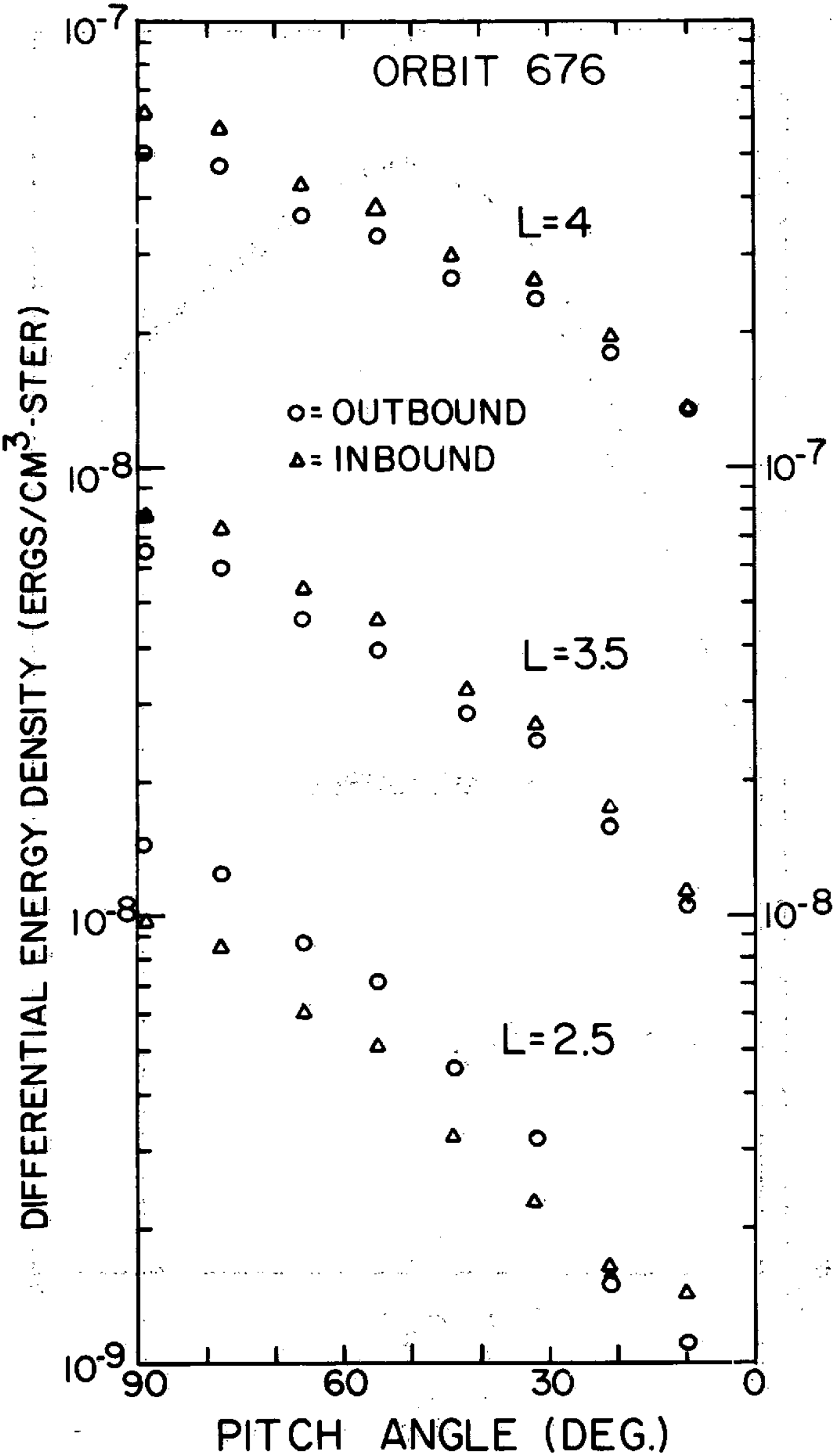
ORBIT 676
L=4
L=3.5
L=2.5
o= OUTBOUND
Δ= INBOUND
DIFFERENTIAL ENERGY DENSITY (ERGS/CM3-STER)
PITCH ANGLE (DEG.)
10-7
10-8
10-8
10-9
10-7
10-8
90
60
30
0

Figure 3

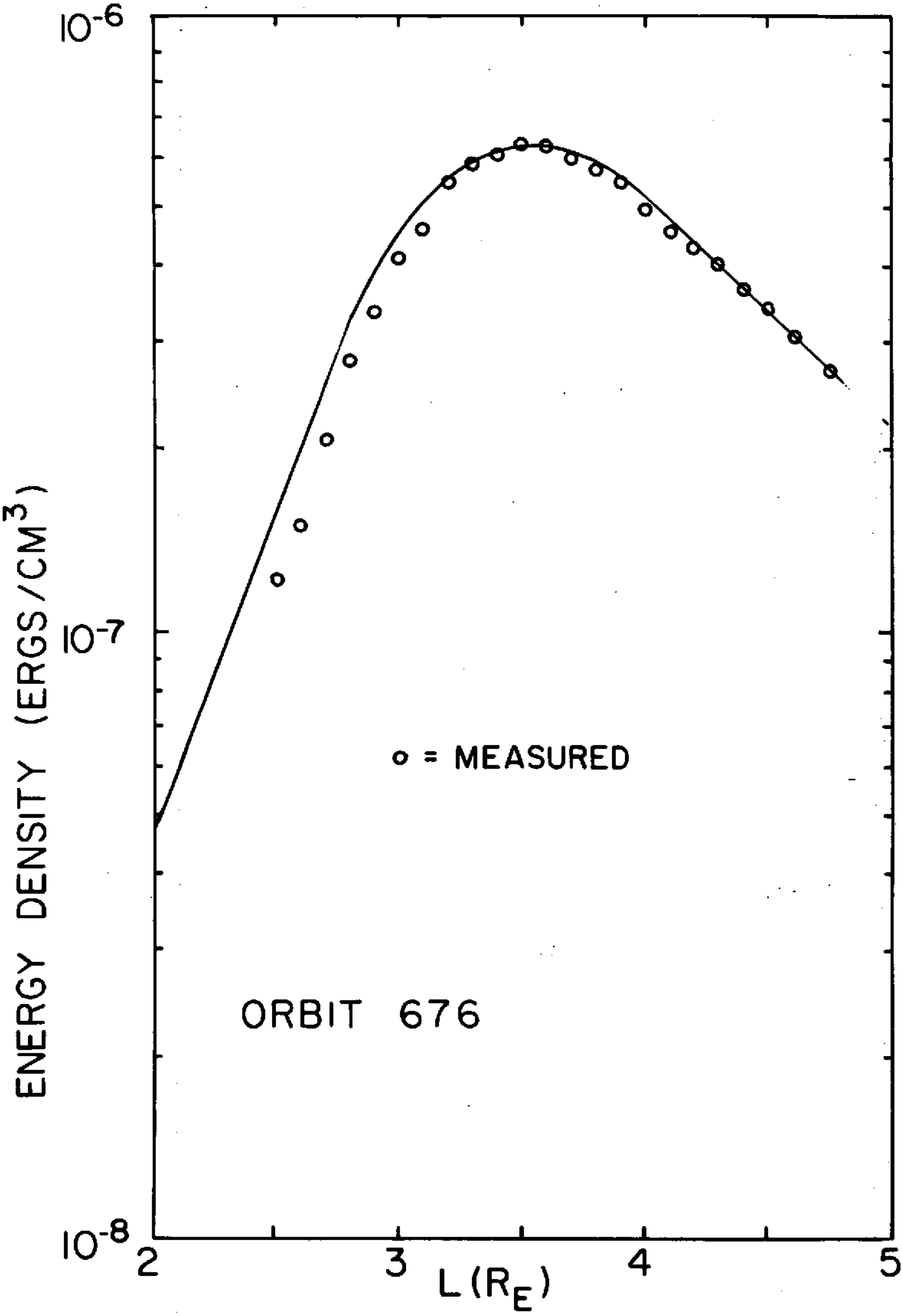
10-6
10-7
10-8
ENERGY DENSITY (ERGS/CM3)
○ = MEASURED
ORBIT 676
2
3
4
5
L(RE)

Figure 4

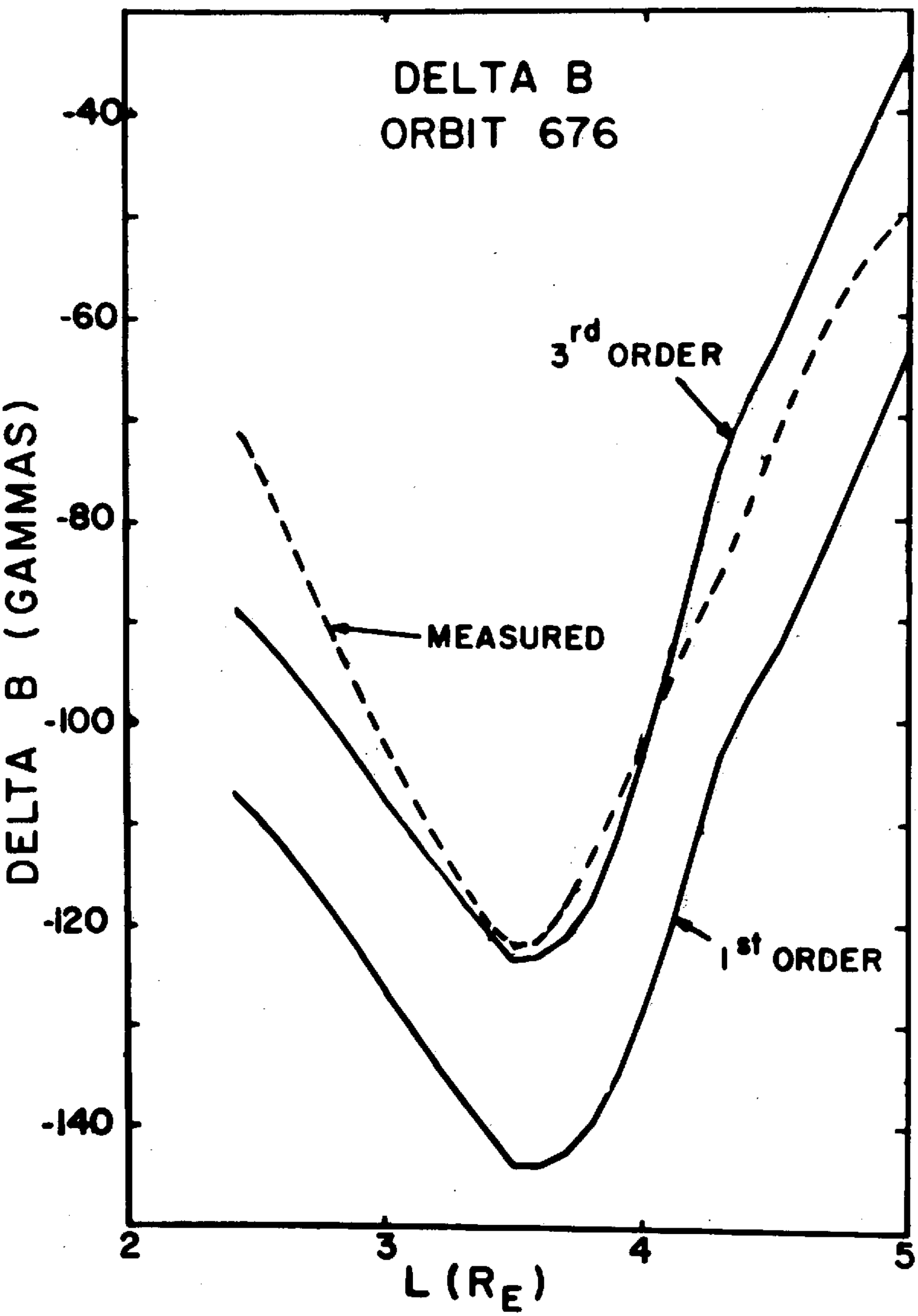

DELTA B
ORBIT 676
-40
-60
-80
-100
-120
-140
DELTA B (GAMMAS)
3rd ORDER
MEASURED
1st ORDER
2
3
4
5
L (R_E)

Figure 5